

Journal Pre-proofs

Crosslinked casein micelles bound paclitaxel as enzyme activated intracellular drug delivery systems for cancer therapy

Julio C. Cuggino, Matías L. Picchio, Agustina Gugliotta, Milagros Bürgi, Ludmila I. Ronco, Marcelo Calderón, Marina Etcheverrigaray, Cecilia I. Alvarez Igarzabal, Roque J. Minari, Luis M. Gugliotta

PII: S0014-3057(20)31954-6
DOI: <https://doi.org/10.1016/j.eurpolymj.2020.110237>
Reference: EPJ 110237

To appear in: *European Polymer Journal*

Received Date: 23 September 2020
Revised Date: 14 December 2020
Accepted Date: 18 December 2020

Please cite this article as: Cuggino, J.C., Picchio, M.L., Gugliotta, A., Bürgi, M., Ronco, L.I., Calderón, M., Etcheverrigaray, M., Alvarez Igarzabal, C.I., Minari, R.J., Gugliotta, L.M., Crosslinked casein micelles bound paclitaxel as enzyme activated intracellular drug delivery systems for cancer therapy, *European Polymer Journal* (2020), doi: <https://doi.org/10.1016/j.eurpolymj.2020.110237>

This is a PDF file of an article that has undergone enhancements after acceptance, such as the addition of a cover page and metadata, and formatting for readability, but it is not yet the definitive version of record. This version will undergo additional copyediting, typesetting and review before it is published in its final form, but we are providing this version to give early visibility of the article. Please note that, during the production process, errors may be discovered which could affect the content, and all legal disclaimers that apply to the journal pertain.

© 2020 Published by Elsevier Ltd.



Crosslinked casein micelles bound paclitaxel as enzyme activated intracellular drug delivery systems for cancer therapy

**Julio C. Cuggino^{1#}, Matías L. Picchio^{2#}, Agustina Gugliotta³, Milagros Bürgi³,
Ludmila I. Ronco¹, Marcelo Calderón^{4,5}, Marina Etcheverrigaray³, Cecilia I.
Alvarez Igarzabal², Roque J. Minari^{1*} and Luis M. Gugliotta^{1*}**

¹⁾ *Instituto de Desarrollo Tecnológico para la Industria Química (INTEC), CONICET-UNL. Güemes 3450. Santa Fe (3000) Argentina.*

²⁾ *Departamento de Química Orgánica, Facultad de Ciencias Químicas, Universidad Nacional de Córdoba, Instituto Investigación en Ingeniería de Procesos y Química Aplicada, IPQA, CONICET-UNC, Haya de la Torre y Medina Allende. Ciudad Universitaria. Córdoba (X5000HUA) Argentina.*

³⁾ *UNL, CONICET, FBCB (School of Biochemistry and Biological Sciences), CBL (Biotechnological Center of Litoral), Ciudad Universitaria, Ruta Nacional 168 – Km 472.4 – C.C. 242 – (S3000ZAA) Santa Fe, Argentina*

⁴⁾ *POLYMAT, Applied Chemistry Department, Faculty of Chemistry, University of the Basque Country UPV/EHU, Paseo Manuel de Lardizabal 3, 20018 Donostia-San Sebastián, Spain*

⁵⁾ *IKERBASQUE, Basque Foundation for Science, 48009 Bilbao, Spain*

These authors contributed equally to this work

*Corresponding authors:

Prof. Dr. Roque J. Minari

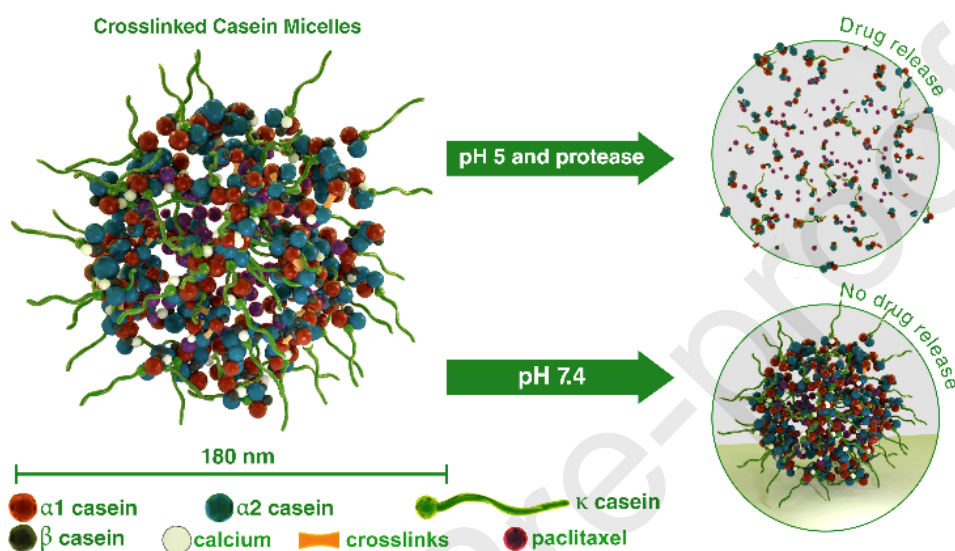
Email: rjminari@santafe-conicet.gov.ar

Prof. Dr. Luis Marcelino Gugliotta

Email: lgug@intec.unl.edu.ar

Keywords: enzyme responsive, casein micelles, drug delivery, cancer therapy, nanomedicine.

Graphical abstract



ABSTRACT

Nanomedicine for cancer therapy is a successful tool to diminish the side effect of chemotherapeutics such as paclitaxel (PTX). In this regard, Abraxane®, a human serum albumin (HSA)-based nanomedicine system has showed lesser side effects than Taxol®. However, the large-scale production of HSA protein is limited and expensive, which is translated in a high cost of the treatments in clinical applications. Thus, the use of easily-available alternative nanocarriers could increment the accessibility of patients to nanomedicine for cancer treatments. Casein is a low-cost protein able to self-assemble into micelles which could efficiently encapsulate PTX into their structure. In this work, the synthesis of chemically crosslinked casein micelles (CCM), used to prepare PTX-based nanoformulations, is presented. CCM@PTX nanoformulations showed promising

results *in vitro* to be applied as nanomedicine for cancer therapy. Thus, the obtained nanoformulations are great candidates to be parenterally administered, accumulate in tumor by passive targeting without leakage of PTX in plasma and release the drug within the tumor microenvironment, in response to overexpressed proteases such as trypsin.

1. Introduction

One of the most used drugs for the chemotherapeutic treatment of various cancer is paclitaxel (PTX), in a formulation called Taxol®.[1] The administration of paclitaxel in chemotherapy is not selective for patients because it affects both normal and cancerous cells. Paclitaxel, a water insoluble drug, requires other excipients for its parenteral administration such as Cremofor®-EL and ethanol. This formulation shows severe adverse effects such as low blood counts, hair loss, peripheral sensory neuropathy, nausea and vomiting, arthralgia, myalgia and extremely hypersensitive reactions.[2] For this reason, with the aim of reducing such undesirable effects and increasing its therapeutic index, paclitaxel has been encapsulated in nanoparticles of different nature such as liposomes [3],[4], polymeric nano/microparticles [5],[6], micelles [7],[8], dendrimers [9],[10], among others.

The encapsulation of paclitaxel in nanoparticles allows directing the drug towards the tumor by the enhanced permeability and retention effect (EPR), also named passive targeting, which was initially described by Maeda.[11] Passive targeting has increased the therapeutic index of paclitaxel, and decreased the doses and adverse effects of Taxol®. One of the products based on nanomedicine and currently approved for use in humans is Abraxane®, consists in a nanoparticle formulation based on human serum albumin (HSA) that encapsulates paclitaxel using nanoparticle albumin bound (NAB)-technology.[1] Another currently commercialized product is a liposomal formulation containing paclitaxel named Lipusu®, which was approved by the State Food and Drug

Administration of China. In addition, the commercialization of other nanosystems based on micelles from a block copolymer of polyethylene glycol (PEG) and polylactic acid (PLA), called Genexol-PM®, has recently been launched.[1] However, all these formulations exhibit problems of nanoparticles stability in blood, since they break into polymer units of lower molecular weight, producing a premature release of the drug in non-specific sites. A possible solution for this problem involves the use of nanovehicles with a crosslinked structure to increase their stability in the bloodstream. After parenteral administration of crosslinked nanoparticles, they can reach the tumor site without drug leakage and then deliver their payload only at the site of action, immediately after facing an environmental trigger. [12],[13],[14]

After approving Abraxane® formulation for human administration, protein-based nanoparticles have received great interest for the encapsulation of PTX.[15–17] However, the high cost of large-scale production of HSA and consequently its use in carriers for cancer therapy, makes this type of products very expensive for the patient. Under this scenario, we have recently proposed the use of bovine casein micelles as alternative nanocarriers of therapeutic drugs.[18],[19] These low-cost vehicles have a hydrophobic core and a hydrophilic surface, present excellent stability in aqueous dispersion and allow for loading a large number of non-polar drugs.[18] In addition, this biodegradable and biocompatible protein has a great number of functional groups which could serve as anchoring points to yield reticulated networks and thus increase the stability of the micelles in dispersion. For this reason, casein is regarded as an excellent candidate as excipient for pharmaceutical applications in drug delivery.[20] Although other authors have previously reported the use of casein micelles (CM) as carriers for oral delivery of PTX in gastric carcinoma therapy [21–26], the parenteral application of this system in cancer therapy has not been reported in literature and could be of great interest for the

pharmaceutical industry. CM are of particular importance due to their nanometric size in dispersion for intracellular drug delivery. The hydrophilic shell of these nanovehicles composed of κ -casein, could mimic PEGylated nanoparticles which are reported to avoid opsonization.[27,28] In addition, CM can be easily degraded by proteolytic enzymes such as trypsin [18] or cathepsin B [29], which are overexpressed in several tumors. Taking into account these theoretical bases, this work proposes the development of stable chemically crosslinked casein micelles (CCM) that contain PTX into their hydrophobic pockets (CCM@PTX), obtaining a novel therapeutic nanoformulation. We prepared and characterized the CCM@PTX nanoformulations and demonstrate their potential to kill cancer cells after activate PTX release by action of trypsin. Thus, after parental administration, the CCM@PTX should be able to transport the anti-tumor drug through the bloodstream, conserving its payload and accumulating in the tumor by the EPR effect. Finally, CCM@PTX could be degraded by proteases in the tumor or intracellular microenvironment, releasing the drug and inhibiting the tumor progression.

2. Experimental section

2.1. Materials and cell lines

The following chemicals were used as purchased: Caseinate sodium salt (CAS, Sigma-Aldrich); N-(3-Dimethylaminopropyl)-N'-ethylcarbodiimide hydrochloride (EDC, Aldrich); N-hydroxysuccinimide (NHS, Aldrich); calcium chloride dihydrate ($\text{CaCl}_2 \cdot 2\text{H}_2\text{O}$, Cicarelli); sodium chloride (NaCl, Cicarelli); acetic acid glacial (AA, Fisher Chemicals); sodium acetate (NaAc, Anedra); sodium dihydrogen phosphate (NaH_2PO_4 , Anedra); disodium hydrogen phosphate (Na_2HPO_4 , Anedra); rhodamine B (RhodB, Aldrich); 0.5% trypsin-EDTA (10X, Gibco); sodium azide (SA, Sigma-Aldrich); sucrose (SC, Sigma-Aldrich); CellTiter 96® AQueous One Solution Cell

Proliferation Assay (MTS/PMS, Promega). Paclitaxel (PTX) was gently supplied by Eriochem S.A from Argentina. HeLa (ATCC® CCL-2™) and PC3 (ATCC® CRL-1435™) cell lines were grown and maintained in Dulbecco's Modified Eagle Medium (DMEM, Gibco) and Dulbecco's Modified Eagle Medium: Nutrient Mixture F-12 (DMEM/F12, Gibco) supplemented with 10 % (v/v) fetal calf serum (FCS, Gibco) and 2 mM glutamine (Gibco), respectively.

2.2 Preparation of CM

CM were prepared according to our previously reported procedure.[18] Briefly, a solution of CAS (50 mg mL⁻¹) was dialyzed against a 0.05 mM CaCl₂ solution for 4 h using a dialysis membrane with molecular weight cut off (MWCO) of 10 kDa. After the dialysis process, re-assembled nanomicelles were kept at 4 °C for 48 h and then centrifuged at 10,000 rpm for 10 min in order to eliminate protein aggregates. Finally, the CM were freeze-dried and stored at 4 °C for the posterior use.

2.3 Synthesis of CCM

In a typical experiment, 40 mL of micelles aqueous dispersion (10 mg/mL) was pre-heated at 70 °C for 10 min. After that, a mixture of EDC and NHS dissolved in 1 mL of water was added with the aim of producing crosslinking between NH₂ and COOH groups of the CAS chains present in the re-assembled CM. Molar ratios of COOH:NHS:EDC = 1:0.25:0.5 and 1:0.5:1 were used aiming to activate 25 and 50% of COOH groups per CAS molecule, respectively. For the calculation, the average molecular weight of casein was regarded 23 kDa as reported in literature [30] and the total number of COOH per molecule was 50, based on the aspartic and glutamic acids residues of this protein. The reaction was carried out at 70 °C for 4 h under stirring conditions. The obtained CCM were dialyzed against ultrapure water (4 changes of water) using a 50 kDa MWCO

membrane. The number of amine groups consumed after the reaction was determined by a colorimetric method using o-phthalaldehyde (OPA) as a fluorescent marker. The OPA method consists in the reaction of this reagent with primary amine groups of proteins to form highly fluorescent 1-alkylthio-2-alkyl substituted isoindoles, which show an absorption band at 340 nm. [31] For the analysis, 100 μL of CM dispersion (1 mg/mL) were mixed with 1 mL of freshly prepared OPA reagent (5 mg of OPA + 100 μL of pure ethanol + 5 μL of 2-mercaptoethanol + 10 mL of 50 mM carbonate buffer pH 10.5). The absorbance was measured at 340 nm by UV-spectroscopy. The crosslinking efficiency was determined according to Eq. 1.

$$\text{Crosslinking efficiency (\%)} = 100 \times (A_{\text{CCM}} - A_{\text{CM}})/A_{\text{CM}} \quad (1)$$

where A_{CM} and A_{CCM} were the absorbance at 340 nm of CM and CCM samples, respectively.

The samples were named CCM0.25 and CCM0.50 according to their theoretical degree of crosslinking.

2.4. Scanning electron microscopy (SEM)

The morphology of the CCM was studied by SEM using a Zeiss Sigma microscope. To this effect, samples were prepared by deposition of 10 μL of CCM (0.001 mg mL⁻¹) onto a silica sheet, covered after drying with chrome in a sputter coater, and observed under an accelerating voltage of 2.0 kV.

2.5 Dynamic light scattering (DLS) characterization

DLS was used to study the resistance of CCM against 0.1 M NaOH (pH 13), as dissociating agent, in order to confirm their crosslinking nature. Measurements were carried out using a Zetasizer Nano ZS (Malvern Instruments) at a scattering angle of 173°

and a laser wavelength of 633 nm. In order that, dispersions of CCM (10 mg mL^{-1}) were diluted 1:5 in 0.01 M NaOH and the size distribution was determined. Non-crosslinked nanomicelles (CM) were used as control. In addition, the hydrodynamic diameters (Z-average) and polydispersity index (PDI) of CCM under simulated physiological and intracellular conditions were also investigated by DLS. Re-dispersions of 1 mg mL^{-1} were prepared in 10 mM phosphate buffer pH 7.4 with 0.14 M NaCl (PBS), or 10 mM acetate buffer pH 5 with 0.14 M NaCl (ABS), and measured at 37°C . Moreover, the degradation of the CCM by proteases was analyzed by DLS following the evolution of Derivate Count Rate (DCR) over time. Thus, CCM dispersions (5 mg mL^{-1}) were diluted 1:5 in PBS (pH 7.4), ABS (pH 5) or ABS (pH 5) plus trypsin (0.05 wt%).

2.6 PTX loading in CCM

PTX was loaded in CCM by hydrophobic interactions. Briefly, a dispersion of CCM (5 mg mL^{-1}) was stirred with PTX previously dissolved in DMSO (10 or 20 wt% based on micelles) for 24 h. Next, micelles dispersion was dialyzed against water for 24 h (MWCO 50 kDa, four replaces of solvent) to eliminate the free PTX and subsequently freeze-dried. The lyophilized powder was then re-dispersed in DMSO for 24 h to extract the loaded drug and centrifuged for the precipitation of the micelles. Finally, the extracted drug was quantified by high performance liquid chromatography (HPLC) using a Waters-Breeze chromatograph fitted with a Waters Symmetry C18 (5 mm, $4.6 \times 150 \text{ mm}$) column and an UV photometer (Waters 2487). A solvent mixture of water/methanol/acetonitrile (25:11:64) was used as mobile phase at 1.0 mL min^{-1} rate. A $20 \mu\text{L}$ injection volume was used, and the PTX detection was performed at 227 nm. Calibration curve was performed using standard solutions of the following concentration: 2.5; 5; 10; 25; 40; 50; and 100 ppm. The Drug Loading Content in the total formulation (%DLC) and the Drug Loading Efficiency (%DLE) were determined according to Eqs. 2 and 3, respectively:

$$\text{DLC (wt \%)} = (W_{\text{DL}} / W_{\text{DLM}}) \times 100 \quad (2)$$

$$\text{DLE (wt \%)} = (W_{\text{DL}} / W_{\text{F}}) \times 100 \quad (3)$$

where W_{DL} is the weight of loaded drug, W_{DLM} is the weight of drug-loaded CCM and W_{F} is the weight of feeding drug.

The CCM@PTX nanoformulations were lyophilized in the dark and then maintained at 4 °C for posterior utilization. The formulations were named CCM0.25@PTX10; CCM0.25@PTX20; CCM0.50@PTX10; and CCM0.50@PTX20. Samples redispersion was realized by sonication for 2 h at 37 °C. For the determination of the hydrodynamic diameter of the loaded samples after re-dispersion, DLS measurements were realized. In addition, the size stability of the CCM@PTX re-dispersions was followed for 7, 19 and 72 h by DLS.

2.7 Thermal analysis of CCM@PTX formulations

The thermal stability of PTX, CCM and CCM@PTX in dry state was studied by thermogravimetric analysis (TGA) on a TGA Q500 thermobalance (TA Instruments). Samples (3 mg) were heated from 25 to 600 °C with a heating rate of 10 °C/min under nitrogen atmosphere (100 mL/min). Analysis by differential scanning calorimetry (DSC) was performed aiming to study the CCM/PTX interaction. Measurements were carried out with a heating rate of 5 °C/min from 25 to 320 °C employing a DSC Q2000 equipment (TA instruments). Dry samples of 8–10 mg were weighed and placed into a hermetic sealed aluminum pan (TZero Technology). Nitrogen was used as purging gas and the sample chamber flushed at a flow rate of 50 mL/min. Thermal transitions were determined using the TA Universal Analysis software.

2.8 Cellular uptake pathways

Different inhibitors were evaluated to study the endocytic uptake mechanisms of CCM. First CCM were labeled with rhodamine B (Rhod B) using EDC/NHS chemistry (the amines of CCM react with the NHS activated carboxylic acid of Rhod B). Then, the effect of the inhibitors was analyzed in HeLa and PC3 culture cells using CCM labeled with Rhod B (CCM-RhodB), as a reporter protein. Cells were seeded in 24-well plate (Greiner, Germany) at a density of 1×10^5 cells per well and incubated at 37 °C for 24 h. The day of the study, cells were pre-incubated under different conditions in order to avoid endocytosis. Two inhibitors were tested at different concentrations: sodium azide (50; 500 and 1000 μ M) and sucrose (0.2; 0.45 and 0.6 M). Since incubation at 4 °C is meant to inhibit endocytosis, this condition was also evaluated. After 1 h of pre-treatment with the corresponding inhibitor, 0.01 mg mL⁻¹ of CCM-RhodB were added to the cells and incubated for 2 h. Cells only treated with CCM-RhodB were included as control of internalization and cells without any treatment (CCM-RhodB and/or inhibitors) as the negative control. Adhered cells were washed 3 times with PBS 1X and analyzed by fluorescence microscopy (Olympus BX-51TRF, Olympus Optical Co. filters Ltd., Tokyo, Japan) equipped with a high-resolution camera (QImaging® Go-3, QImaging, Surrey, BC, Canada). Treatments were performed by duplicate and five pictures of each biological replicate, were taken, in order to perform the statistical analysis, using the same settings according to the excitation intensity. Images were processed by the plugins of Image J software to determine the mean fluorescence intensity (MFI). More than twenty cells per image were analyzed. Data collected was normalized with CCM-RhodB control and expressed as endocytosis inhibition percentage. Statistical analysis was carried out using one-way ANOVA followed by Dunnett's test.

2.9 In vitro cell toxicity

In vitro cytotoxicity assays were performed in order to determine the non-toxic limit concentration (NLTC) of blank-CCM and the IC₅₀ of CCM@PTX. Briefly, HeLa and PC3 cells were seeded into culture microtiter plates (Greiner, Germany) using growth medium at a density of 2.5×10^4 cells per well and incubated at 37 °C overnight. The culture supernatants were removed and serial dilutions of the samples CCM0.25 and CCM0.50 in growth medium were accomplished. CCM0.25 and CCM0.50 were evaluated in a concentration range from 0.5 to 0.008 mg mL⁻¹ for both cell lines. PTX as well as CCM0.25@PTX10, CCM0.25@PTX20, CCM0.50@PTX10 and CCM0.50@PTX20 were evaluated from 100 nM to 0.8 nM of PTX for both cell lines. Cells without treatment were used as growth control. Plates were incubated at 37 °C for 24 and 48 h. Cell proliferation was determined using a CellTiter 96™ Aqueous Non-Radioactive Cell Proliferation Assay (Promega). Absorbance was read at 492 and 690 nm using a microplate reader (Multiskan™, Thermo Fisher Scientific). Absorbance of CCM was plotted against its concentration (mg mL⁻¹). In the case of CCM loaded with PTX, plots of absorbance against PTX concentration (nM) were graphed. The IC₅₀ was determined from CCM@PTX graphs as the concentration of the micelle that produces the death of the fifty percent of the culture while NLTC was calculated for the blank-CCM as the highest concentration which produced the same color intensity than that of the negative control. The assays were carried out in four independent times and triplicates of the samples were evaluated in each test. Statistical analysis was carried out using Student's t test or one-way ANOVA followed by Tukey's post-test, accordingly.

3. Results and Discussion

3.1 Preparation of CCM

The CCM were prepared using the intrinsic properties of CAS to form micelles followed by a crosslinking process. Therefore, the synthesis of CCM was carried out through a two-step method as shown schematically in Figure 1. First, CM were re-assembled by dialysis in the presence of CaCl_2 . [18] In this step, the hydrodynamic diameter of the micelles formed was 163.3 nm (PDI = 0.116) as determined by DLS. After that, aiming to confer structural stability to the CM, an intra-micellar crosslinking reaction was performed between NH_2 and COOH groups present in the protein molecule. As it is widely known, amines could react with acid groups that were previously activated by EDC/NHS chemistry. The crosslinking reaction was carried out at 70 °C since the PDI (0.086) of CM at this temperature was considerably lower than that at 25 °C (PDI= 0.228), as it was determined by DLS analysis under controlled temperature. CCM were obtained as a white dispersion after 4 h of reaction. As first evidence referred to the effectiveness of the crosslinking reaction, the whitish dispersion obtained for CCM did not return to the most transparent white color of the CM after cooling at 25 °C. The number of amine groups consumed after the reaction determined by a colorimetric method using OPA as an fluorescent marker. Crosslinking efficiencies of 21% and 50% were obtained for CCM0.25 and CCM0.5, respectively.

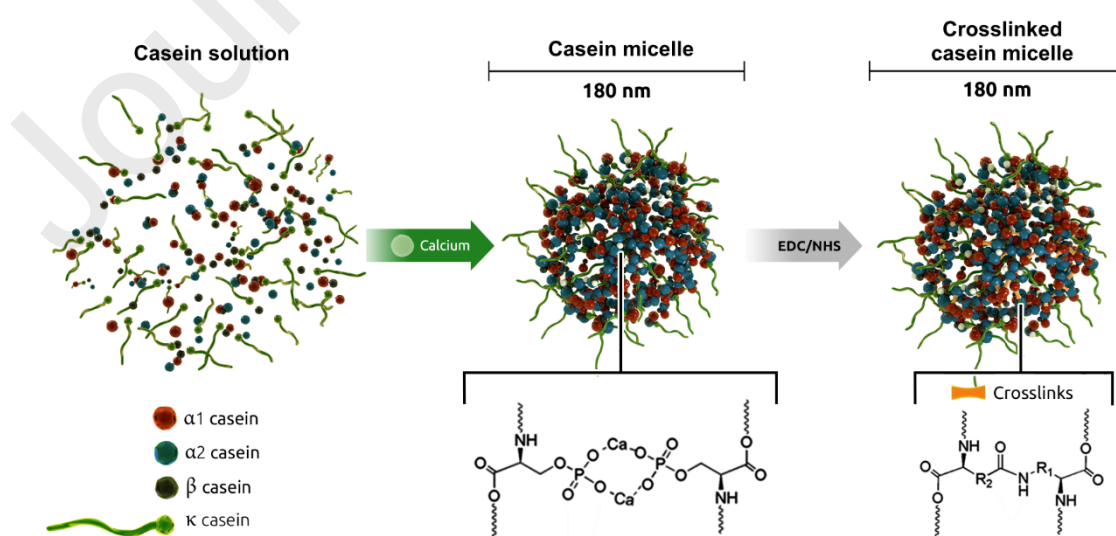


Figure 1. Schematic representation of CCM preparation.

3.2 CCM stability determined by DLS

In order to study the stability of the chemically crosslinked structure generated after micelles formation and amine/carboxylic acid intra-micellar reaction, the size distributions of the CCM were determined by DLS against 0.1 M NaOH (pH 13) as dissociating agent. Figure 2 shows the intensity-based size distribution of CCM0.50 in water or strong alkaline conditions, and compared with CM in the same media.

As it can be observed, CCM resulted stable at pH 13 maintaining the size distribution with only small increase in the hydrodynamic diameter, probably due to the action of the dissociating agent which increases the swelling of the crosslinked structure. In contrast, CM were easily disassembled at pH 13, because the strong alkaline conditions disrupt the cohesive interactions between the hydrophobic region of the CAS.[32] CCM0.25 also showed high stability in alkaline medium as it can be observed in Figure S1 of the Supporting Information (SI). However, size distribution resulted broader for CCM0.25 than for CCM0.5, which suggest that micelles present lower number of crosslinked points in accordance with the less amount of NHS/EDC couple used for their preparation (see Figure S2 in SI). These results show that CCM could be attractive as carriers in drug delivery for cancer therapy. Indeed, CCM could maintain the structural integrity in plasma conditions until achieving tumor tissue by EPR effect, thus preventing a premature drug release in a non-specific site.

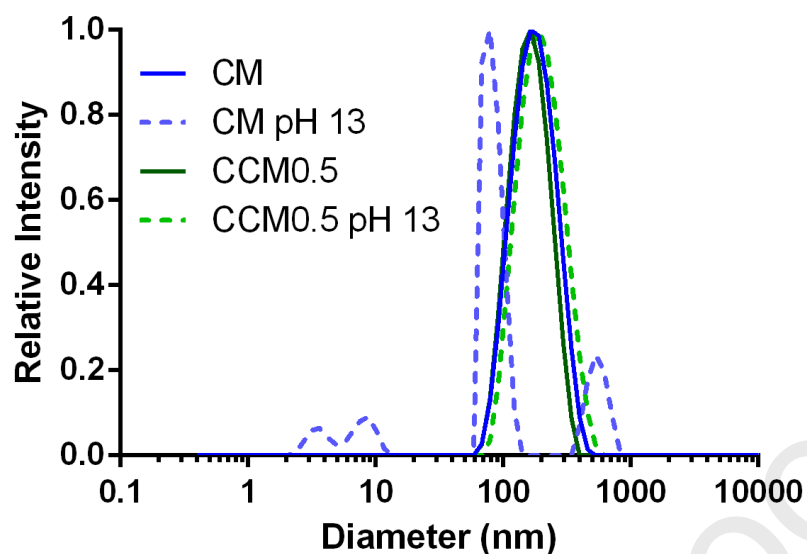


Figure 2. Intensity-based size distribution of NonCM and CCM0.50 in water or alkaline conditions.

3.3 SEM characterization

The morphology of therapeutic nanocarriers is a key parameter to consider since it influences in their cellular uptake and penetration inside tumor tissue. Recent studies demonstrated that spherical nanoparticles show a significantly higher cell internalization than rods and vesicles.[33] Thus, the shape and size of CCM were analyzed by SEM. Figure 3 shows micrographies obtained for CCM0.50. As it can be observed, CCM present spherical morphology with a size of approximately 100 nm in dry state.

a)

b)

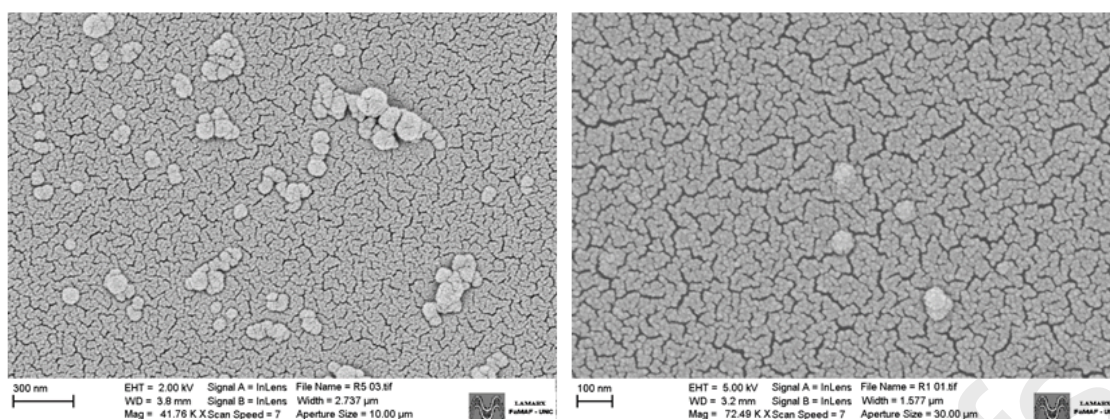


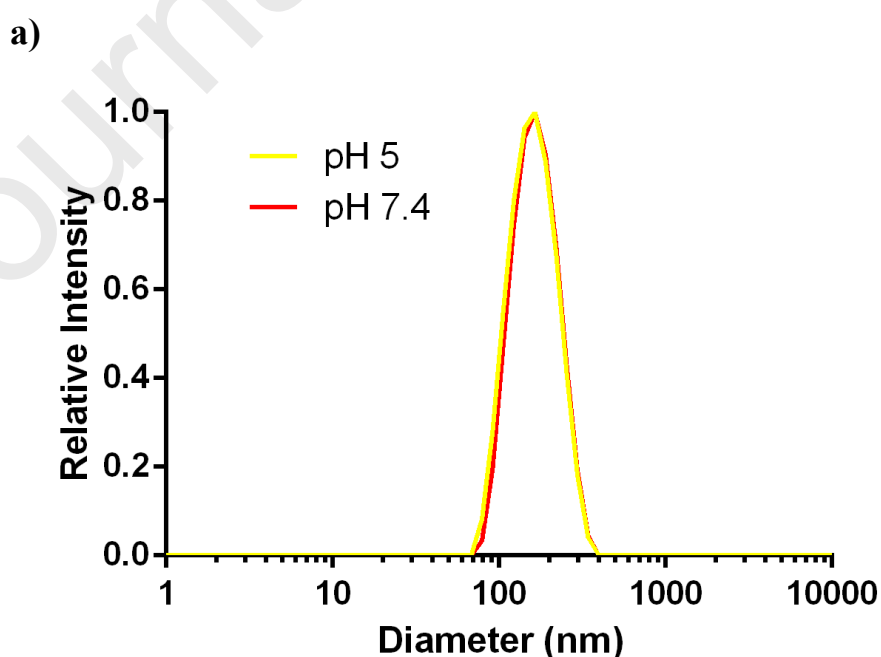
Figure 3. Morphology of CCM0.50 observed by SEM at different magnifications.

3.4 Hydrodynamic diameter and enzymatic degradation of CCM in physiological media

As it is known, the size and stability of nanoparticles under physiological salt concentrations and different pH conditions could define their utility as nanovehicles. The nanoparticle size is a crucial parameter that must be controlled to avoid the rapid clearance of the nanocarriers from the body by the reticuloendothelial system (RES) or by renal filtration. Thus, the hydrodynamic diameter of CCM was determined simulating the conditions that they would face during blood circulation and cellular internalization pathways. The micelles presented unimodal distributions (see Figures 4a and S3 of the SI) with similar diameters at both pH 7.4 and pH 5 (both under 0.14 M NaCl), without evidence of disintegration under these conditions. The mean sizes of CCM0.25 and CCM0.50 were 176.2 (PDI 0.101) and 190.0 nm (PDI 0.126) at pH 7.4; and 169.2 (PDI 0.128) and 182.9 nm (PDI 0.119) at pH 5, respectively. A small increase in the size of both CCM was observed at pH 7.4 in comparison with pH 5, since micelles are probably more negatively ionized at nearly neutral pH (the isoelectric point of CAS is 4.6) inducing charge repulsion and producing an increased swelling of the network. However, the diameters of CCM at physiological pH and salt concentration are appropriated for their utilization in cancer therapy. As it is widely accepted for the scientific community,

nanoparticles with sizes below 5 nm are rapidly cleared by renal filtration, while sizes smaller than 200 nm are less phagocytosed by the RES.

Since casein-based micelles could be susceptible to proteases overexpressed in tumor microenvironment (TME) or intracellular conditions, the degradation capability using trypsin as model protease was analyzed. To this effect, the evolution of the derivate count rate (DCR) of micelles in dispersion, after enzyme addition, was followed over time by DLS.[34] As it can be observed in Figure 4b, the micelles were degraded immediately after the addition of trypsin in the medium, which is evidenced by the tremendous decrease of the DCR (light scattering intensity) from approximately 270000 to 70000 kcps with almost not variations in the size of CCM (176.7 to 162.6 nm). These results suggest that under TME or cancer intracellular conditions, where proteases such as trypsin or cathepsin B are overexpressed, the enzyme activity could trigger an immediate release of any payload due to the disintegration of CCM structure.



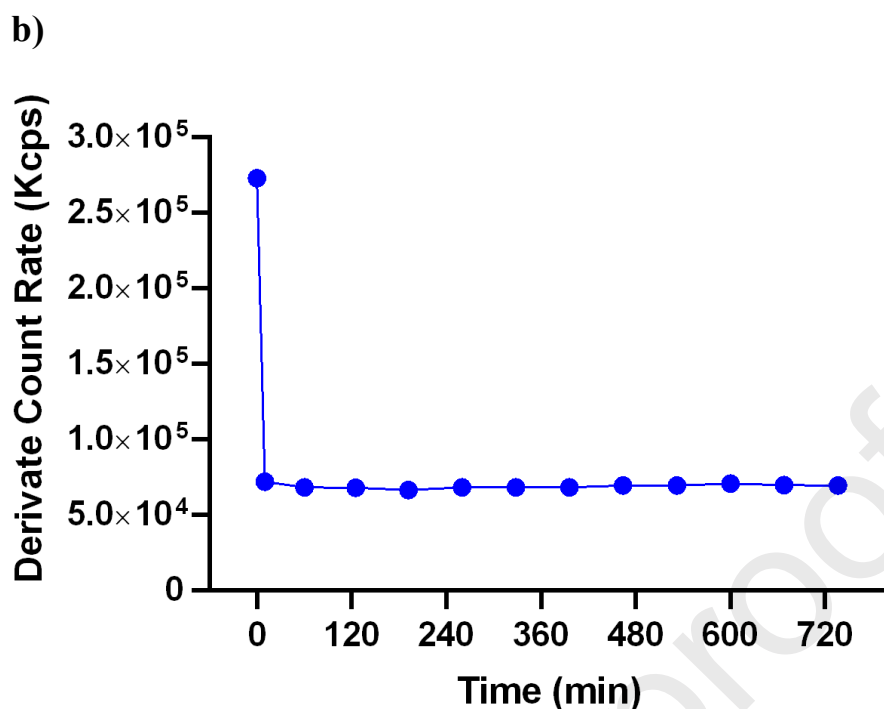


Figure 4. a) Intensity-based size distribution of CCM0.50 in simulated physiological media at 37 °C; and b) evolution of the derived count rate of CCM0.50 after trypsin addition.

3.7 Loading of PTX within the CCM

The encapsulation of a highly hydrophobic drug, as PTX, in aqueous medium remains a challenge for nanocarriers engineering in pharmaceutical technology. In general, the nanocarrier should present a hydrophilic shell to interact with water and a hydrophobic core which could encapsulate the drug. In this regard, the amphiphilic nature of CCM, allows the effective encapsulation of PTX in aqueous dispersion as is schematically shown in Figure 5.

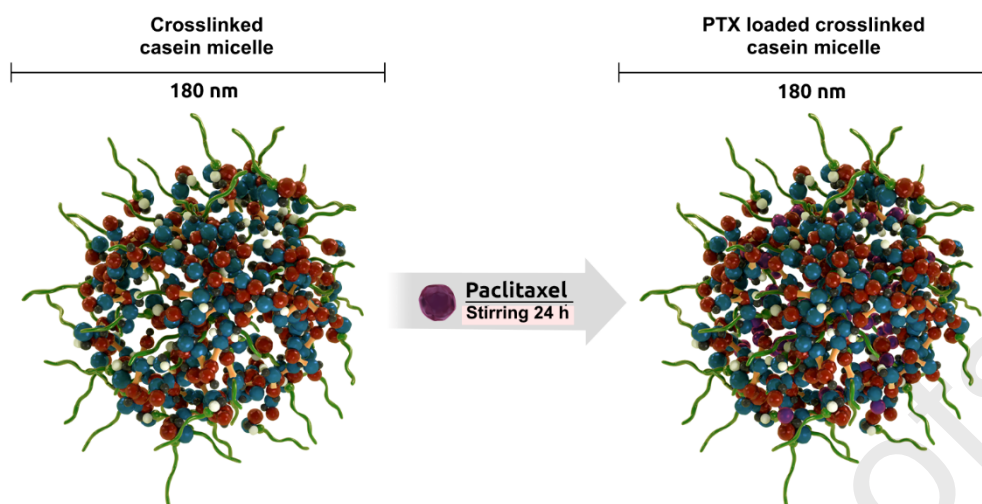


Figure 5. Schematic representation of PTX loading in CCM

After the addition of solid PTX to the CCM dispersion, the drug kept insoluble, but with 24 h of stirring, it was completely dissolved by the interaction with the hydrophobic pockets of the protein. Stable formulations with % DLC of 10 or 20 were prepared reaching 100% of DLE, as determined by HPLC analysis. The micelles increased 180 times the solubility of PTX in water (the solubility values of PTX in water and in CCM dispersion, are $0.00556 \text{ mg mL}^{-1}$, and 1 mg mL^{-1} , respectively). The re-dispersion of the micelles after lyophilization was performed by sonication. Thus, after 2 h of sonication at $37 \text{ }^{\circ}\text{C}$, the micelles were able to recover their original size as was determined by DLS (Table 1).

Table 1: Hydrodynamic diameter of the micelles after lyophilization and 2 h of sonication for re-dispersion.

Sample	Size (nm) and PDI after lyophilization and re-dispersion
CCM0.25	176 (0.175)
CCM0.25@PTX10	172 (0.208)
CCM0.25@PTX20	220 (0.165)

CCM0.50	189 (0.123)
CCM0.50@PTX10	259 (0.187)
CCM0.50@PTX20	224 (0.175)

After loading and lyophilization process, the CCM@PTX formulations were analyzed by DSC in order to verify the interaction between CCM and PTX. The DSC thermogram of CCM0.25@PTX10 was compared with those from CCM0.25, pure PTX, and a physical mixture of CCM0.25 and PTX, as shown in Figure 6. As it can be observed, CCM0.25 showed a glass transition temperature at 135 °C and a sharp endothermic peak at 153.1 °C which correspond to thermal degradation of casein [35]. PTX presented an endothermic peak at 213 °C corresponding to its melting point. The physical mixture of CCM and PTX displayed similar peaks observed in the pure components with a slight decrease in the PTX melting point (201 °C). However, for CCM@PTX formulation, the melting endothermic peak of PTX at 213 °C was not present, suggesting that the drug loading in CCM was effective. Similar results were observed for CCM0.50@PTX formulation (see Figure S4 of the SI).

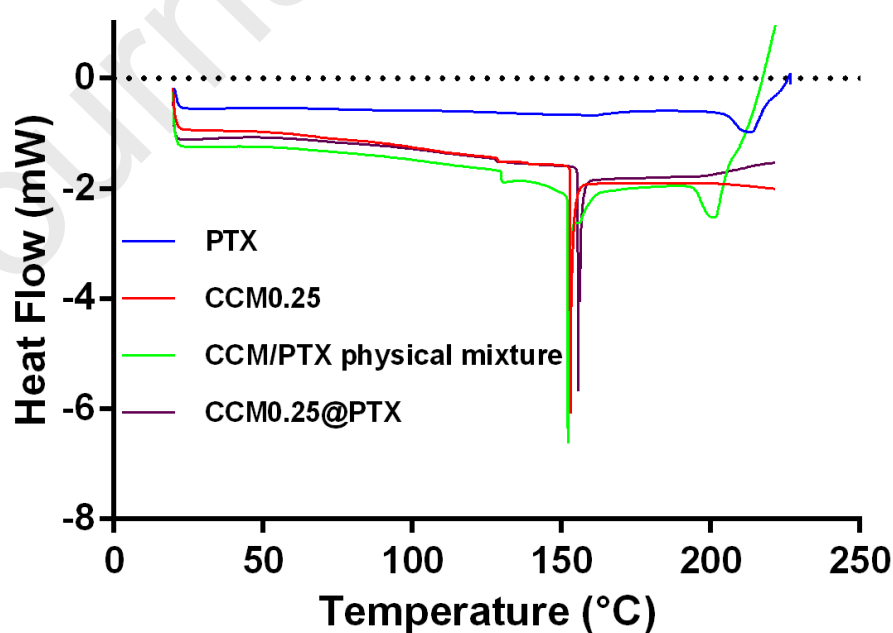


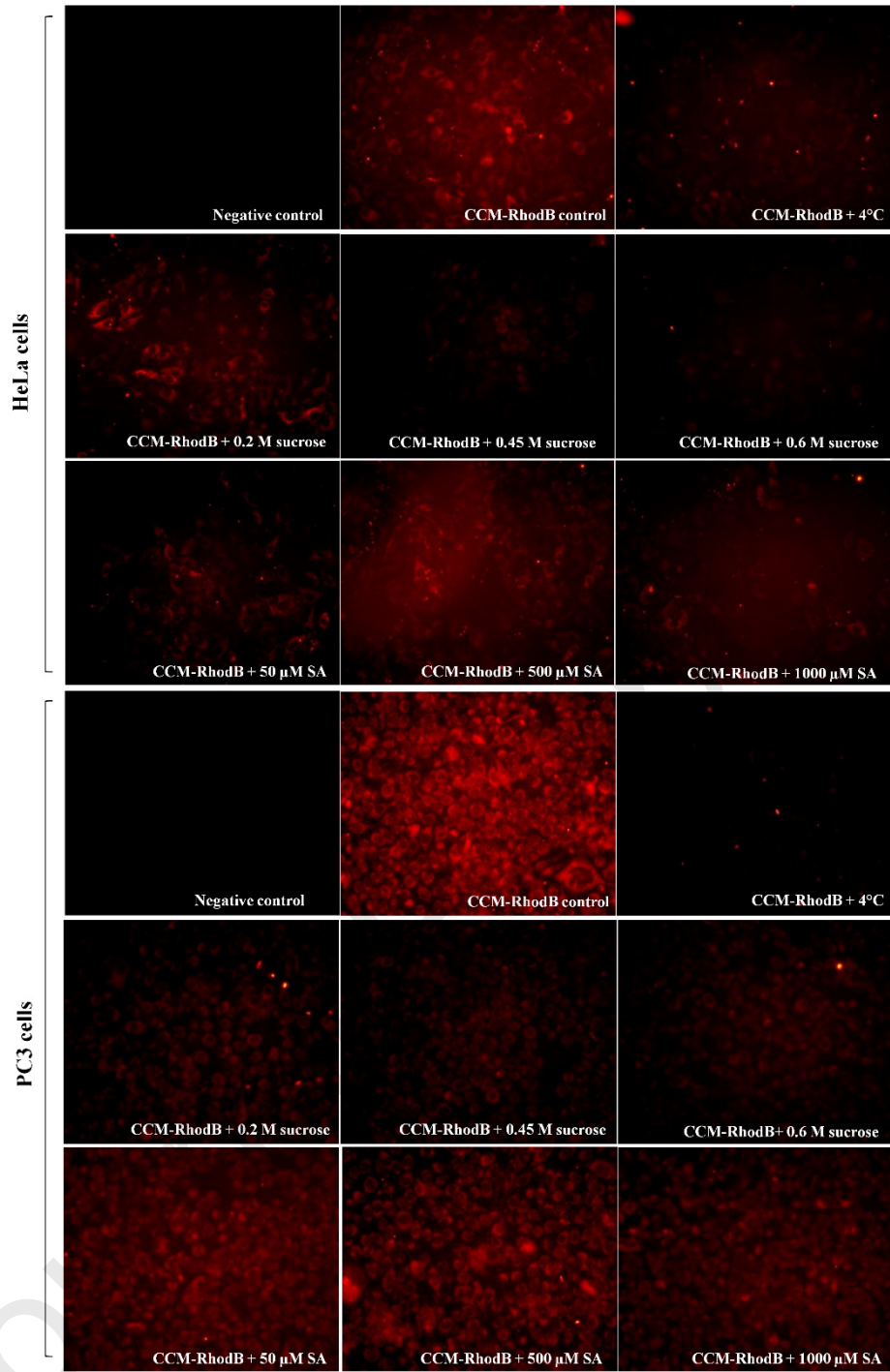
Figure 6. DSC thermograms of CCM0.25@PTX10 formulation compared with non-loaded CCM0.25, PTX and CCM0.25/PTX physical mixture.

3.8 Cellular uptake pathways of CCM

Cellular uptake analysis of CCM-RhodB was studied by fluorescence microscopy in the cancer cell lines HeLa and PC3. Different endocytosis pathways were inhibited using varied conditions and inhibitor concentrations. So, different experimental conditions were used: sucrose, as an inhibitor of clathrin-mediated endocytosis; sodium azide, as an inhibitor of energy depending endocytosis and temperature at 4 °C as an inhibitor of all energy-dependent pathways were used. Thus, fluorescence microscopy images were taken after incubation of cells with CCM-RhodB 0.01 mg mL⁻¹ at different endocytosis inhibitor conditions, and the corresponding mean fluorescence intensity (MFI) was obtained. As it is shown in Figure 7a, the fluorescence intensity of the cells was notably reduced after 4 °C-incubation. The same effect was observed after incubation with increasing concentrations of sucrose and sodium azide. Those results evidence that inhibitors lower the entrance of CCM-RhodB to both cell lines. The MFI data obtained from the images were normalized to determine the percentage of endocytosis inhibition for each treatment. Thus, cells incubated only with CCM-RhodB (normal uptake control) were considered as 0% inhibition and the statistical analysis was performed (Figure 7b). The percentage of endocytosis inhibition was higher for PC3 cells reaching up to 60% values while the maximum inhibition percentage for HeLa cells was up to 40%. This result indicates that PC3 cells are more susceptible to the treatments. Sodium azide and sucrose treatments showed a dose-dependent inhibition effect for both cell lines. The different concentrations of both inhibitors used in this assay were previously analyzed to confirm that they are not toxic for PC3 and HeLa cells. Particularly, incubation at 4 °C

was also effective to reduce the entrance of CCM-RhodB to both cell lines. Specifically, for PC3 cells all the conditions studied showed statistical significance compared to the control (CCM-RhodB), while for HeLa cells only 4 °C, sodium azide 1000 µM and sucrose 0.45 and 0.6 M presented a significant inhibition effect. These results indicate that CCMs are uptaken by PC3 and HeLa cells through different endocytosis pathways. Particularly, the notable inhibition observed after the incubation of CCM-RhodB with sucrose in PC3, suggests that the clathrin endocytosis pathway might present a protagonist role.

a)



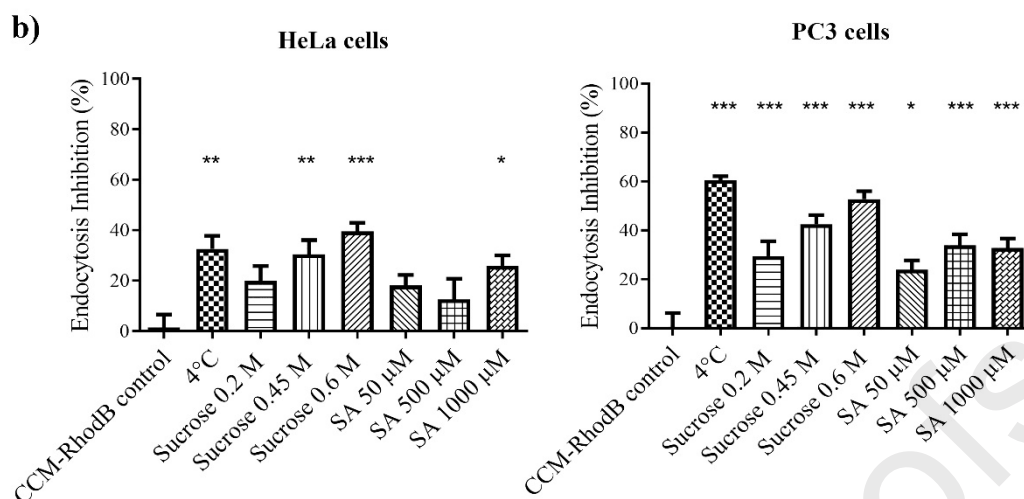


Figure 7: Cellular uptake in HeLa and PC3 cells after incubation of CCM-RhodB and different endocytosis inhibitors for 2 h. a) Fluorescence microscopy images of HeLa and PC3 cells treated with CCM-RhodB in presence of different endocytosis inhibitors: temperature (4 °C); 0.2, 0.45, 0.6 M sucrose and 50, 500, 1000 µM sodium azide (SA). Negative control represents cells without any treatment. b) The MFI data from the images were normalized and used for the determination of the endocytosis inhibition percentage as: $100 - ((\text{MFI sample}/\text{MFI control}) * 100)$. Statistical analysis was carried out using one-way ANOVA followed by Dunnett's test. * $p < 0.05$; ** $p < 0.01$; *** $p < 0.001$ represent the degree of statistical significance.

3.9 Cell viability

Initially, *in vitro* biological assays were performed in order to determine the cytotoxicity of blank CCM against HeLa and PC3 cells, after 24 and 48 h of incubation. As it can be observed in Table 1a, CCM0.5 shows significantly higher toxicity than CCM0.25 for both cell lines ($p < 0.05$). Particularly, the NTLC of CCM0.5 corresponds to half of the value observed for CCM0.25 for both periods of incubation studied, indicating that the former is doubly toxic. This behavior could be attributed to the major degree of crosslinking which creates a more rigid structure for CCM0.5 diminishing their biodegradability and

affecting the cell viability. Later, the IC₅₀ of CCM@PTX was studied on the same cell lines and periods of incubation. The IC₅₀ was calculated considering the concentration of PTX (nM). To compare the toxicity between unloaded micelles and CCM@PTX, the concentration of the micelle (ng mL⁻¹) corresponding to each IC₅₀, was calculated. The result from the *in vitro* biological assays revealed that all the CCM@PTX exhibited cytotoxicity in a dose-dependent manner as well as free PTX. Besides, the NTLC of the blank CCM resulted in the order of μg mL⁻¹ and the corresponding IC₅₀ of loaded micelles (based on the IC₅₀ regarding to the PTX content) resulted in the order of ng mL⁻¹. So it could be confirmed that the toxicity of CCM@PTX is inherent to the PTX content and is not related with the composition of the micelles. After 24 h of incubation, it can be observed that HeLa cells are more susceptible to PTX than PC3, since the IC₅₀ is significantly lower in this cell line (p=0.0014), meaning that lower concentrations are enough to induce cytotoxicity. The statistical analysis of the results obtained after testing CCM@PTX in PC3 cells reveals that the nanoformulations are significantly more cytotoxic than free PTX (p<0.05), except for CCM0.50@PTX20 that did not show significant differences after 24 h of incubation. In the case of HeLa cells, PTX loaded micelles resulted as cytotoxic as PTX (no significant differences). The only exception was CCM0.50@PTX20 since it showed lower cytotoxicity after 24 h of incubation. In general, if the PTX-loaded micelles were compared, the CCM0.25 seems to be more toxic than the CCM0.5 since their IC₅₀ is inferior, meaning that a lower concentration of CCM0.25 can be used to induce cytotoxicity in both cell lines. Particularly, the IC₅₀ of CCM0.25@PTX20 was significantly lower compared to CCM0.5@PTX20 (p<0.05), supporting the idea mentioned above. This result might be due to the micelles composition and probably, the higher toxicity of CCM0.25 could be associated with a better release of PTX from the micelles than CCM0.5 because of the minor degree of

crosslinking points increases the degradability. Furthermore, comparing CCM0.25@PTX10 with CCM0.25@PTX20 pairs, the former exhibits higher cytotoxicity. This can be observed when comparing all the 10 and 20 CCM@PTX pairs. A certain difficulty for PTX release can be observed for the CCM containing a higher PTX loading. Taken together, the comparison of micelles with different characteristics, CCM0.25@PTX10 vs. CCM0.5@PTX20, revealed that the lower the crosslinking degree and the PTX loading, the higher the cytotoxicity ($p < 0.05$) for both cell lines. Altogether, these results show the potential of the nanoformulations to be used in cancer therapy. Specifically, CCM0.25@PTX10 represents an interesting candidate since it can to induce cytotoxicity in PC3 and HeLa cells using the lowest concentration, and could reduce the side effects that this type of treatments could provoke in the patients.

Table 2: NTLC of CCM and IC50 of CCM@PTX and free PTX in HeLa and PC3 cells after 24 and 48 h of incubation.

a) NTLC of unload CCM

NTLC of CCM ($\mu\text{g ml}^{-1}$)							
Sample	PC3			HeLa			Time of incubation
CCM0.25	126	\pm	25	78	\pm	15	24 h
CCM0.5	64	\pm	17	45	\pm	25	
CCM0.25	83	\pm	29	167	\pm	23	48 h
CCM0.5	38	\pm	2	73	\pm	6	

b) IC50 of CCM@PTX and free PTX

Sample	IC50 of PTX and		CCM concentration		Time of incubation
	CCM@PTX (nM)		(ng mL ⁻¹) *		
	PC3	HeLa	PC3	HeLa	
PTX	11 ± 2	2 ± 1	-	-	
CCM0.25@PTX10	4.4 ± 0.1	3 ± 1	38 ± 1	26 ± 9	
CCM0.5@PTX10	6.4 ± 0.3	5 ± 2	55 ± 3	43 ± 17	
CCM0.25@PTX20	5 ± 1	5 ± 2	21 ± 4	21 ± 9	24 h
CCM0.5@PTX20	10 ± 2	8 ± 3	43 ± 9	34 ± 13	
PTX	11 ± 2	8 ± 2	-	-	
CCM0.25@PTX10	4 ± 1	5 ± 1	34 ± 9	43 ± 9	
CCM0.5@PTX10	3.4 ± 0.5	7 ± 2	29 ± 4	60 ± 17	
CCM0.25@PTX20	5 ± 1	6 ± 1	21 ± 4	26 ± 4	48 h
CCM0.5@PTX20	6 ± 3	7.5 ± 0.3	26 ± 13	32 ± 1	

The IC₅₀ of each sample (PTX and CCM@PTX) was calculated considering the concentration of PTX (nM). For each IC₅₀ calculated in columns 2 and 3, the corresponding concentration of micelles in ng mL⁻¹ was determined (*columns 4 and 5).

4. Conclusions

Crosslinked casein micelles (CCM) were effectively prepared in two steps with diameters of approximately 180 nm in dispersion and spherical morphology. An immediate degradability of the micelles against trypsin was observed by DLS. The CCM were able to load 10 and 20 wt% of PTX in a simple procedure without compromising the

dispersability of the micelles. A good interaction between the micelles and PTX was shown by DSC analysis. The main pathway for cell uptake of the CCM was the clathrin-mediated endocytosis, as demonstrated by fluorescence microscopy using different inhibitors. In addition, cell toxicity studies in two cancer cell lines showed that the CCM@PTX formulations were more cytotoxic than free PTX. Thus, the nanoformulations could present potential for their parenteral administration with a posterior accumulation in tumor microenvironment by passive targeting (EPR effect) and producing enzyme-activated release of PTX to kill cancer cells. Finally, these preliminary results encourage us to think that the prepared low-cost nanomedicine could be an alternative in cancer therapy to the marketed Abraxane®.

5. Acknowledgments

The authors gratefully acknowledge financial support of ANPCyT, CONICET, UNL, and UNC from Argentina; IKERBASQUE- Basque Foundation for Science and MINECO via the project RTI2018-099227-B-I00 from Spain. In addition, the authors would like to acknowledge Eriochem SA for Paclitaxel donation.

6. References

- [1] National Cancer Institute, Natl. Cancer Inst. (2020).
- [2] Chemocare, Chemocare, Chemocare. (2020).
- [3] P. Crosasso, M. Ceruti, P. Brusa, S. Arpicco, F. Dosio, L. Cattel, Preparation, characterization and properties of sterically stabilized paclitaxel-containing liposomes, *J. Control. Release.* 63 (2000) 19–30.
doi:[https://doi.org/10.1016/S0168-3659\(99\)00166-2](https://doi.org/10.1016/S0168-3659(99)00166-2).

- [4] S.-T. Huang, Y.-P. Wang, Y.-H. Chen, C.-T. Lin, W.-S. Li, H.-C. Wu, Liposomal paclitaxel induces fewer hematopoietic and cardiovascular complications than bioequivalent doses of Taxol, *Int. J. Oncol.* 53 (2018) 1105–1117.
doi:10.3892/ijco.2018.4449.
- [5] F. Danhier, N. Lecouturier, B. Vroman, C. Jérôme, J. Marchand-Brynaert, O. Feron, V. Préat, Paclitaxel-loaded PEGylated PLGA-based nanoparticles: In vitro and in vivo evaluation, *J. Control. Release.* 133 (2009) 11–17.
doi:https://doi.org/10.1016/j.jconrel.2008.09.086.
- [6] M. Cegłowski, J. Kurczewska, P. Ruszkowski, G. Schroeder, Application of paclitaxel-imprinted microparticles obtained using two different cross-linkers for prolonged drug delivery, *Eur. Polym. J.* 118 (2019) 328–336.
doi:https://doi.org/10.1016/j.eurpolymj.2019.06.010.
- [7] A.W. Du, H. Lu, M.H. Stenzel, Core-Cross-Linking Accelerates Antitumor Activities of Paclitaxel–Conjugate Micelles to Prostate Multicellular Tumor Spheroids: A Comparison of 2D and 3D Models, *Biomacromolecules.* 16 (2015) 1470–1479. doi:10.1021/acs.biomac.5b00282.
- [8] Y. Dai, L. Zhang, R. Xiang, Y. Wan, X. Pan, L. Zheng, Y. Yin, H. Zheng, Y. Yi, Polymeric micelles with photo-activated proton release behavior for enhanced tumor extracellular pH targeting and drug release, *Eur. Polym. J.* 96 (2017) 69–78. doi:https://doi.org/10.1016/j.eurpolymj.2017.08.039.
- [9] E.N. Cline, M.-H. Li, S.K. Choi, J.F. Herbstman, N. Kaul, E. Meyhöfer, G. Skiniotis, J.R. Baker, R.G. Larson, N.G. Walter, Paclitaxel-Conjugated PAMAM Dendrimers Adversely Affect Microtubule Structure through Two Independent Modes of Action, *Biomacromolecules.* 14 (2013) 654–664.

doi:10.1021/bm301719b.

- [10] H. Bhatt, S.V. Kiran Rompicharla, B. Ghosh, V. Torchilin, S. Biswas, Transferrin/ α -tocopherol modified poly(amidoamine) dendrimers for improved tumor targeting and anticancer activity of paclitaxel, *Nanomedicine*. 14 (2019) 3159–3176. doi:10.2217/nnm-2019-0128.
- [11] Y. Matsumura, H. Maeda, A New Concept for Macromolecular Therapeutics in Cancer Chemotherapy: Mechanism of Tumoritropic Accumulation of Proteins and the Antitumor Agent Smancs, *Cancer Res*. 46 (1986) 6387 LP-6392.
- [12] S. Wang, P. Huang, X. Chen, Stimuli-Responsive Programmed Specific Targeting in Nanomedicine, *ACS Nano*. 10 (2016) 2991–2994. doi:10.1021/acsnano.6b00870.
- [13] Z. Jiang, J. Chen, L. Cui, X. Zhuang, J. Ding, X. Chen, Advances in Stimuli-Responsive Polypeptide Nanogels, *Small Methods*. 2 (2018) 1700307. doi:doi:10.1002/smt.201700307.
- [14] L. Zhang, Y. Wang, X. Zhang, X. Wei, X. Xiong, S. Zhou, Enzyme and Redox Dual-Triggered Intracellular Release from Actively Targeted Polymeric Micelles, *ACS Appl. Mater. Interfaces*. 9 (2017) 3388–3399. doi:10.1021/acsmi.6b14078.
- [15] B.B. Mandal, S.C. Kundu, Self-assembled silk sericin/poloxamer nanoparticles as nanocarriers of hydrophobic and hydrophilic drugs for targeted delivery, *Nanotechnology*. 20 (2009) 355101. doi:10.1088/0957-4484/20/35/355101.
- [16] T.K. Yeh, Z. Lu, M.G. Wientjes, J.L.-S. Au, Formulating Paclitaxel in Nanoparticles Alters Its Disposition, *Pharm. Res*. 22 (2005) 867–874. doi:10.1007/s11095-005-4581-4.

- [17] Z. Jin, Y. Lv, H. Cao, J. Yao, J. Zhou, W. He, L. Yin, Core-shell nanocarriers with high paclitaxel loading for passive and active targeting, *Sci. Rep.* 6 (2016) 27559.
- [18] M.L. Picchio, J.C. Cuggino, G. Nagel, S. Wedepohl, R.J. Minari, C.I. Alvarez Igarzabal, L.M. Gugliotta, M. Calderón, Crosslinked casein-based micelles as a dually responsive drug delivery system, *Polym. Chem.* 9 (2018) 3499–3510. doi:10.1039/c8py00600h.
- [19] J.C. Cuggino, F.E. Ambrosioni, M.L. Picchio, M. Nicola, Á.F. Jiménez Kairuz, G. Gatti, R.J. Minari, M. Calderón, C.I. Alvarez Igarzabal, L.M. Gugliotta, Thermally self-assembled biodegradable poly(casein-g-N-isopropylacrylamide) unimers and their application in drug delivery for cancer therapy, *Int. J. Biol. Macromol.* 154 (2020). doi:10.1016/j.ijbiomac.2020.03.138.
- [20] A.O. Elzoghby, W.S. Abo El-Fotoh, N.A. Elgindy, Casein-based formulations as promising controlled release drug delivery systems, *J. Control. Release.* 153 (2011) 206–216. doi:10.1016/j.jconrel.2011.02.010.
- [21] M. Bar-Zeev, Y.G. Assaraf, Y.D. Livney, β -casein nanovehicles for oral delivery of chemotherapeutic Drug combinations overcoming P-glycoprotein-mediated multidrug resistance in human gastric cancer cells, *Oncotarget.* 7 (2016) 23322–23334. doi:10.18632/oncotarget.8019.
- [22] M. Bar-Zeev, L. Nativ, Y.G. Assaraf, Y.D. Livney, Re-assembled Casein Micelles for Oral Delivery of Chemotherapeutic Combinations to Overcome Multidrug Resistance in Gastric Cancer, *J. Mol. Clin. Med.* (2018). doi:10.31083/j.jmcm.2018.01.008.

- [23] A. Shapira, Y.G. Assaraf, D. Epstein, Y.D. Livney, Beta-casein Nanoparticles as an Oral Delivery System for Chemotherapeutic Drugs: Impact of Drug Structure and Properties on Co-assembly, *Pharm. Res.* 27 (2010) 2175–2186. doi:10.1007/s11095-010-0222-7.
- [24] A. Shapira, Y.G. Assaraf, Y.D. Livney, Beta-casein nanovehicles for oral delivery of chemotherapeutic drugs, *Nanomedicine Nanotechnology, Biol. Med.* 6 (2010) 119–126. doi:https://doi.org/10.1016/j.nano.2009.06.006.
- [25] A. Shapira, I. Davidson, N. Avni, Y.G. Assaraf, Y.D. Livney, β -Casein nanoparticle-based oral drug delivery system for potential treatment of gastric carcinoma: Stability, target-activated release and cytotoxicity, *Eur. J. Pharm. Biopharm.* 80 (2012) 298–305. doi:https://doi.org/10.1016/j.ejpb.2011.10.022.
- [26] A. Shapira, G. Markman, Y.G. Assaraf, Y.D. Livney, β -casein-based nanovehicles for oral delivery of chemotherapeutic drugs: drug-protein interactions and mitoxantrone loading capacity, *Nanomedicine Nanotechnology, Biol. Med.* 6 (2010) 547–555. doi:https://doi.org/10.1016/j.nano.2010.01.003.
- [27] C.G. de Kruif, E.B. Zhulina, κ -casein as a polyelectrolyte brush on the surface of casein micelles, *Colloids Surfaces A Physicochem. Eng. Asp.* 117 (1996) 151–159. doi:https://doi.org/10.1016/0927-7757(96)03696-5.
- [28] A.O. Elzoghby, M.W. Helmy, W.M. Samy, N.A. Elgindy, Novel ionically crosslinked casein nanoparticles for flutamide delivery: formulation, characterization, and in vivo pharmacokinetics, *Int. J. Nanomedicine.* 8 (2013) 1721–1732. doi:10.2147/IJN.S40674.
- [29] T. Considine, Á. Healy, A.L. Kelly, P.L.H. McSweeney, Hydrolysis of bovine

- caseins by cathepsin B, a cysteine proteinase indigenous to milk, *Int. Dairy J.* 14 (2004) 117–124. doi:[https://doi.org/10.1016/S0958-6946\(03\)00171-7](https://doi.org/10.1016/S0958-6946(03)00171-7).
- [30] W.N. Eigel, J.E. Butler, C.A. Ernstrom, H.M. Farrell, V.R. Harwalkar, R. Jenness, R.M.L. Whitney, *Nomenclature of Proteins of Cow's Milk: Fifth Revision*, *J. Dairy Sci.* 67 (1984) 1599–1631. doi:10.3168/jds.S0022-0302(84)81485-X.
- [31] V.J. Svedas, I.J. Galaev, I.L. Borisov, I. V Berezin, The interaction of amino acids with ophthaldialdehyde: a kinetic study and spectrophotometric assay of the reaction product., *Anal. Biochem.* 101 (1980) 188–195. doi:10.1016/0003-2697(80)90059-7.
- [32] B. Vaia, M.A. Smiddy, A.L. Kelly, T. Huppertz, Solvent-Mediated Disruption of Bovine Casein Micelles at Alkaline pH, *J. Agric. Food Chem.* 54 (2006) 8288–8293. doi:10.1021/jf061417c.
- [33] J. Zhao, H. Lu, S. Wong, M. Lu, P. Xiao, M.H. Stenzel, Influence of nanoparticle shapes on cellular uptake of paclitaxel loaded nanoparticles in 2D and 3D cancer models, *Polym. Chem.* 8 (2017) 3317–3326. doi:10.1039/C7PY00385D.
- [34] J. Trousil, S.K. Filippov, M. Hrubý, T. Mazel, Z. Surová, D. Cmarko, S. Svidenská, J. Matějková, L. Kováčik, B. Porsch, R. Konefał, R. Lund, B. Nyström, I. Raška, P. Štěpánek, System with embedded drug release and nanoparticle degradation sensor showing efficient rifampicin delivery into macrophages, *Nanomedicine Nanotechnology, Biol. Med.* 13 (2017) 307–315. doi:<https://doi.org/10.1016/j.nano.2016.08.031>.
- [35] M. Corzo-Martínez, M. Mohan, J. Dunlap, F. Harte, Effect of Ultra-High

Pressure Homogenization on the Interaction Between Bovine Casein Micelles and Ritonavir, *Pharm. Res.* 32 (2015) 1055–1071. doi:10.1007/s11095-014-1518-9.

Highlights

- Cross-linked casein micelles (CCM) were prepared using casein self-assembly properties
- The CCM were degraded immediately after exposition to proteases
- The CCM were able to load paclitaxel (PTX) in their structure
- *In vitro* studies in models cells showed that CCM@PTX improve the toxicity of PTX
- CCM@PTX have potential for parenteral administration to treat cancers with proteases overexpression